

Measurement of wood surface roughness in *Dinizia excelsa* Ducke using an atomic force microscope

Willian Silva da Conceição¹, Robert Saraiva Matos^{2,3}, Ituanany da Costa Melo¹, Glenda Quaresma Ramos⁴, Fidel Guereiro Zayas¹ and Henrique Duarte da Fonseca Filho^{1*}

¹Laboratório de Síntese de Nanomateriais e Nanoscopia, Departamento de Física, Universidade Federal do Amazonas, Av. General Rodrigo Octavio Jordão Ramos, 1200, 69067-005, Manaus, Amazonas, Brasil. ²Programa de Pós-Graduação em Ciência e Engenharia de Materiais, Universidade de Sergipe, São Cristóvão, Sergipe, Brasil. ³Grupo de Materiais da Amazônia, Departamento de Física, Universidade Federal do Amapá, Macapá, Amapá, Brasil. ⁴Programa de Pós-Graduação em Medicina Tropical, Fundação de Medicina Tropical Doutor Heitor Vieira Dourado, Universidade Estadual do Amazonas, Manaus, Amazônia, Brasil. *Author for correspondence. E-mail: henriquedffilho@yahoo.com.br

ABSTRACT. Measurement techniques of nanoscale parameters have been vastly explored nowadays. In systems such as wood that possess anisotropic surfaces, these techniques provide reliable data on the surface morphology and related parameters. The atomic force microscope (AFM) and optical microscope were used to investigate the roughness and surface morphology of *Dinizia excelsa*. Cuts were made in different directions generating three distinct surfaces: radial, tangential and transverse. The samples went through a sanding process to reveal the original morphology of the steering. Both techniques show that the surface texture is different according to the analysed surface. The lowest roughness was observed on the transverse plane while the highest occurred on the radial. The comparison of the morphology evaluation by the two techniques allowed us to see that the AFM technique revealed the most sensitive images in smaller scales. These results confirmed that the AFM can provide satisfactory results for the surface parameters of *Dinizia excelsa* depending on the cut direction. This type of analysis can be useful in laboratory species identification processes and in deforestation inspection processes in the Amazon.

Keywords: Wood; *Dinizia excelsa*; AFM; morphology; roughness.

Received on November 4, 2020.
 Accepted on December 18, 2020.

Introduction

Angelim Pedra or Vermelho (*Dinizia excelsa*) that belongs to the Leguminosae or Fabaceae family is a tree often found in the Amazon rainforest, particularly in Brazil, in the states of Amazonas, Acre, Amapá, Mato Grosso, Pará, Rondônia. It includes 727 genus and 19,325 species, being the third largest family among angiosperms, and in Brazil, they are represented by about 2,100 native species, gathered in 188 genus distributed in almost all plant formations, which vary between large trees, shrubs, herbs and creepers (Lewis, Schrire, Mackinder, & Lock, 2005). It is a tree that can reach 55 meters height, allowing straight and cylindrical trunk and a density that varies between 0.95 g cm⁻³ – 1.00 g cm⁻³ (Oliveira, Cesarino, Pantoja, & Môro, 2010). It is a great asset for the timber and construction industry due to its endurance and resistance to attack by termites, fungi, and other wood parasites (Alday, Gómez, Ojeda, Caballero, & Moneo, 2005). Depending on the region, it has several popular names such as angelim, angelim-amarelo, angelim-da-mata, angelim-do-pará, mirarema, angelim-macho (Corrêa, 1974). Its wood has a heartwood and sapwood distinguished by color, whether or not it is light or dark brown, with darker brown spots due to the oozing of oil-resin, while the sapwood is pale brown in color (Mainieri & Primo, 1968). Another characteristic is that it does not shine. Its smell and taste are imperceptible; it shows an average density, hard on cutting, and coarse texture of the fibrous aspect (Ferreira, Gomes, & Hopkins, 2004).

It is known that, since it is composed of cellulose, hemicellulose, lignin polymers and has specific anatomical shapes, woods are capable of removing or yielding moisture to the environment, as it is a heterogeneous, anisotropic and hygroscopic material. These characteristics are explained by their chemical constitution, in addition to external growth conditions, such as climate, soil, among others. Thus, the region of origin and the anatomical direction considered determine the physical, chemical, and mechanical

properties (Martins, 1988). The anatomy of wood is an area of botanical science that seeks to understand the structural arrangement of its various constituent elements. As the main purpose, the study of the wood anatomy has, undoubtedly, a microscopic recognition of the wood. The advantages resulting from this identity certification are of real scope for trading and the timber industry. Their anatomical examination represents the only safe way to identify them (Moreschi, 2005). Due to its anisotropic structure, the performances shown in the radial, tangential and transverse directions are different. Moreschi (2005) states that the greatest dimensional change is manifested first in the tangential direction, then in the radial direction, and finally in the transverse direction, which, by being so low, it is usually neglected in practice (Moreschi, 2005).

Reliable results in a study on wood involve two approaches to the anatomical identification: the macroscopic, where little or no magnification is needed, and the microscopic using optical microscopes with magnifications up to 1000 times. For larger magnifications, generally, scanning electron microscopy (SEM) and atomic force microscopy (AFM) are two of the most suitable techniques for high resolution surface analysis, each of which resolves characteristics on the sample surface even with scales up to 10 nm (Ghisleni, Rzepiejewska-Malyska, Philippe, Schwaller, & Michler, 2009; Kawasaki et al., 2017; Melling, Karimian-Teherani, Mostler, Behnam, & Hochmeister, 2004).

The macroscopic structure of the wood has characteristics that are divided into two groups: organoleptic and anatomical. Organoleptic (or sensory) include: color, shine, odor, taste, grain, texture, density, hardness, and designs. It is characterized by the shapes, sizes, and concentrations of parenchyma cells, distributed in different ways, generally functioning as starch deposits visible to the naked eye, or with a magnifying glass up to ten times. In microscopic identification, the characteristics of the tissues and cells that make up the wood are observed, which are not distinct without the use of a microscope, such as: type of punctuation, cell wall ornamentation, cell composition of rays, cell dimensions, presence of crystals, etc. (Botosso, 2009).

The roughness of the surface depends on several factors related to the structure and anatomical properties of the wood, the machining tools, and the cutting parameters used. The properties of wood that affect roughness are density, moisture content, texture, and anatomical structure (Aguilera & Muñoz, 2011; Csanády, Magoss, & Tolvaj, 2015; Gurau, Mansfield-Williams, & Irle, 2005). Normally profilometers are used to calculate the roughness of this type of material. However, AFM appears as an alternative to perform this type of measurement with high sensitivity and resolution. Although roughness is one of the parameters used to characterize wood, studies in the literature using the AFM technique for this purpose are rare. Thus, in this study, we present the results of the superficial analysis of Angelim Pedra wood, cut in anatomical faces by means of R_q (mean square roughness) and R_a (arithmetic mean roughness) roughness, in addition to AFM topographic images.

Material and methods

The species was selected based on data from the forest inventory of the management plan for the area and on the results of research on the woods mainly used in the region for commercial timber purposes. In this study, Angelim Pedra came from a native forest management plan located on the AM 010 road, Km 188 ME Urubu, Itacoatiara-AM, Brazil, under the geographical coordinates: latitude 02°52'27.95204"; longitude 58°59'12.45495".

Sample preparation

The material was collected in the forest storage yard, where it was cut into small logs (discs) 35 cm long in the direction of the fibers and, for that, trees with a diameter greater than 50 cm were chosen. These logs were processed with the aid of a circular saw and a planer, resulting into cubes with dimensions of: 2 cm x 2 cm x 2 cm in length, width, and thickness, respectively (Figure 1), cut in three anatomical directions: radial, tangential and transverse. The specimens represent a line of 10 spacings between the center and sapwood, with 10 replications, totaling 100 specimens for the species studied.

After being cut on the three surfaces (Radial, Transverse, and Tangential) the woods surfaces were sanded by a 1200 grid sand paper to become more suitable for scanning with the AFM, without the probe touching the sample easily so that it was not damaged. Therefore, these three samples were labeled as R, Tr, and, Ta (Radial, Transverse, and Tangential, respectively). Then, the samples were taken into an ultrasonic washer, which is a device designed to assist in cleaning samples, removing all dirt and impurities found on the surface

and in the smallest and deepest recesses. After using the ultrasound, a laboratory oven at a temperature (45°C) was used, so that the water remaining in the samples was completely evaporated. After the procedure, the samples were ready for analysis by atomic force microscopy.

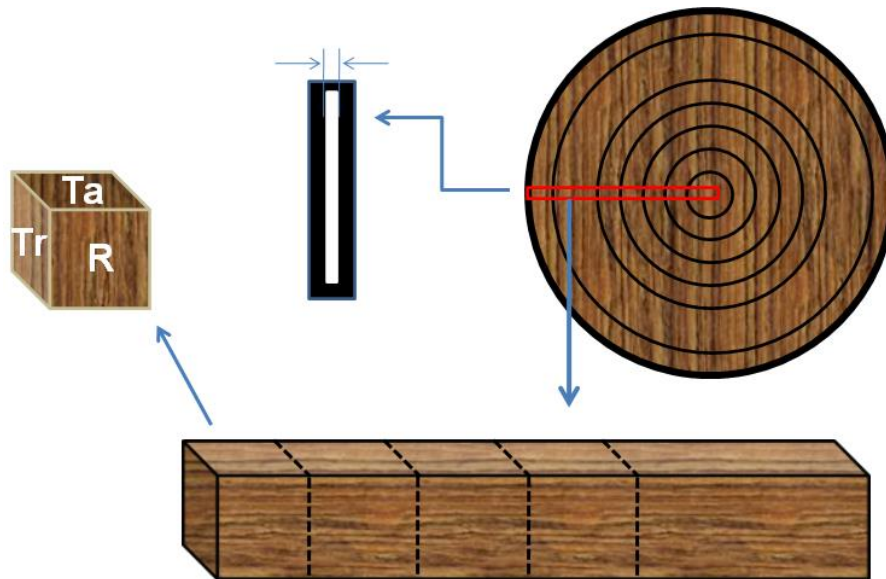


Figure 1. Scheme of cutting the samples for analysis on log by AFM.

Experimental procedure with AFM

An Innova AFM model from Bruker (Santa Barbara, CA, USA) was used in tapping mode to perform the ultrastructural characterization of surfaces. Five different regions of each sample were measured with areas of $10\ \mu\text{m} \times 10\ \mu\text{m}$ and resolution of 256×256 pixels using a silicon cantilever, performed at a scan rate of 0.5 Hz. All measurements were accomplished in the air, at room temperature ($296 \pm 1\ \text{K}$) and $40 \pm 1\ \%$ relative humidity, and the feedback control was adapted to each surface to obtain the best images. In order to seek more suitable regions for the study here proposed, the optical microscope attached to the AFM was used.

The analysis of the images was completed with the WSXM software, version 5.0, development 9.1 (Horcas et al., 2013) and, through the images, it is possible to obtain the surface roughness. The arithmetic mean roughness of the surface is one of the parameters universally used, and is defined as the absolute mean deviation of irregularities in the roughness of the midline over a length of the surface (Abouelatta & Mádl, 2001). R_a is defined as (Gadelmawla, Koura, Maksoud, Elewa, & Soliman, 2002):

$$R_a = \frac{1}{N_x N_y} \sum_{i=1}^{N_x} \sum_{j=1}^{N_y} |z(i, j) - z_{mean}| \quad (1)$$

where

$$z_{mean} = \frac{1}{N_x N_y} \sum_{i=1}^{N_x} \sum_{j=1}^{N_y} z_{ij} \quad (2)$$

and N_x and N_y represent the number of points on the x and y axes, respectively. The mean square roughness is the standard deviation of the surface height distribution and is used to describe the surface roughness using statistical methods, being calculated by the Equation (Gadelmawla et al., 2002):

$$R_q = \sqrt{\frac{1}{N_x N_y} \sum_{i=1}^{N_x} \sum_{j=1}^{N_y} (z(i, j) - z_{mean})^2} \quad (3)$$

It is important to note that, comparatively R_q is more susceptible to large deviations from the midline of the surface. The roughness values were calculated from five different AFM topography non-contact mode scans with a sharp tip (radius $< 20\ \text{nm}$) for each cut direction. The original AFM data were levelled by mean plane subtraction before roughness calculation, without further correction of the flatten filter, and the same tip was used for different locations.

Results and discussion

The micrographs resulting from the investigation are presented in Figure 2 and to compare macroscopically, a top view of the samples is also shown. As it can be easily observed, each cut direction exhibits a different texture.

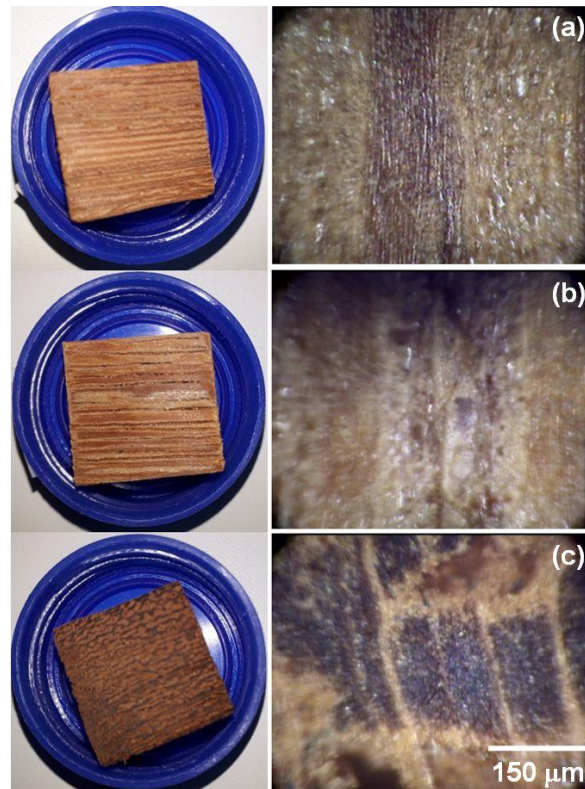


Figure 2. Optical microscopy images comparing the surfaces of the (a) radial, (b) tangential, and (c) transverse sections and a top view of the samples, respectively cut into cubes.

During the cutting process, several anatomical parts of the wood are separated and the properties of the separated parts are influenced by the grain pattern and the physical and mechanical properties of the wood. This causes a change in the micro-geometry of the surface making it heterogeneous (Thoma, Peri, & Lato, 2015). Due to its cellular structure, the cut surface of wood consists of diverse components and hollow spaces, as shown in Figure 2.

Electron microscopy, which includes Scanning and Transmission Electron microscopy (SEM and TEM, respectively) techniques, is commonly used to study wood structures that are either too small to be observed by naked eye or too small/irregular to be viewed using optical microscopy. They are able to reach great magnification as compared with optical microscopy, such as 1 million times or more. TEM can be used to study the internal structure (ultrastructure) of biological samples such as wood and wood undergoing biodegradation. TEM is a technique through which a beam of electrons accelerated from an electron source (similar to SEM) is transmitted through ultrathin specimens (usually < 100 nm) providing information that can be visualized. However, both techniques have limitations with respect to the samples and require a specific preparation before the measurements, particularly in the case of TEM (Daniel, 2016). On the other hand, AFM, another microscopy technique used here, can magnify up to a billion times and it uses a tip or probe which touches the sample surface point by point. The tip deflexion is interpreted as the surface topography by the software, producing 2D or 3D images that generate several tribological parameters such as roughness in respect to a scanned area, being a promising tool for studying biological materials (Cybulska, Konstankiewicz, Zdunek, & Skrzypiec, 2010; Romagnoli, Sarlatto, Terranova, Bizzarri, & Cesetti, 2007; Zhang et al., 2012).

Figure 3 shows the AFM images of $10\ \mu\text{m} \times 10\ \mu\text{m}$ of each type of cut made in the wood, where the images in two dimensions correspond to the amplitude channel (which is the derivative of the topography image in the scanning direction) and, the three dimensions are the respective topographies. The analysis

of the amplitude images seemed better for the visualization and observation of the nanoscale wood texture. Figure 3 also shows the profile of a line on each surface.

Areas with artificial risks must be avoided when performing the AFM scan, since these areas can not represent the actual surface morphology of the wood and may be the residue of the sanding process. Besides, these inadequate regions could damage the AFM tip. Therefore, before scanning, it is important to choose the best area using an optical microscope (Figure 2). The original images were rendered by the software on a color scale in which the darker regions are related to the valleys or holes in the sample, while the more yellowish regions represent peak regions. On the other hand, regions with whiter colors represent a saturation of the heights in the images.

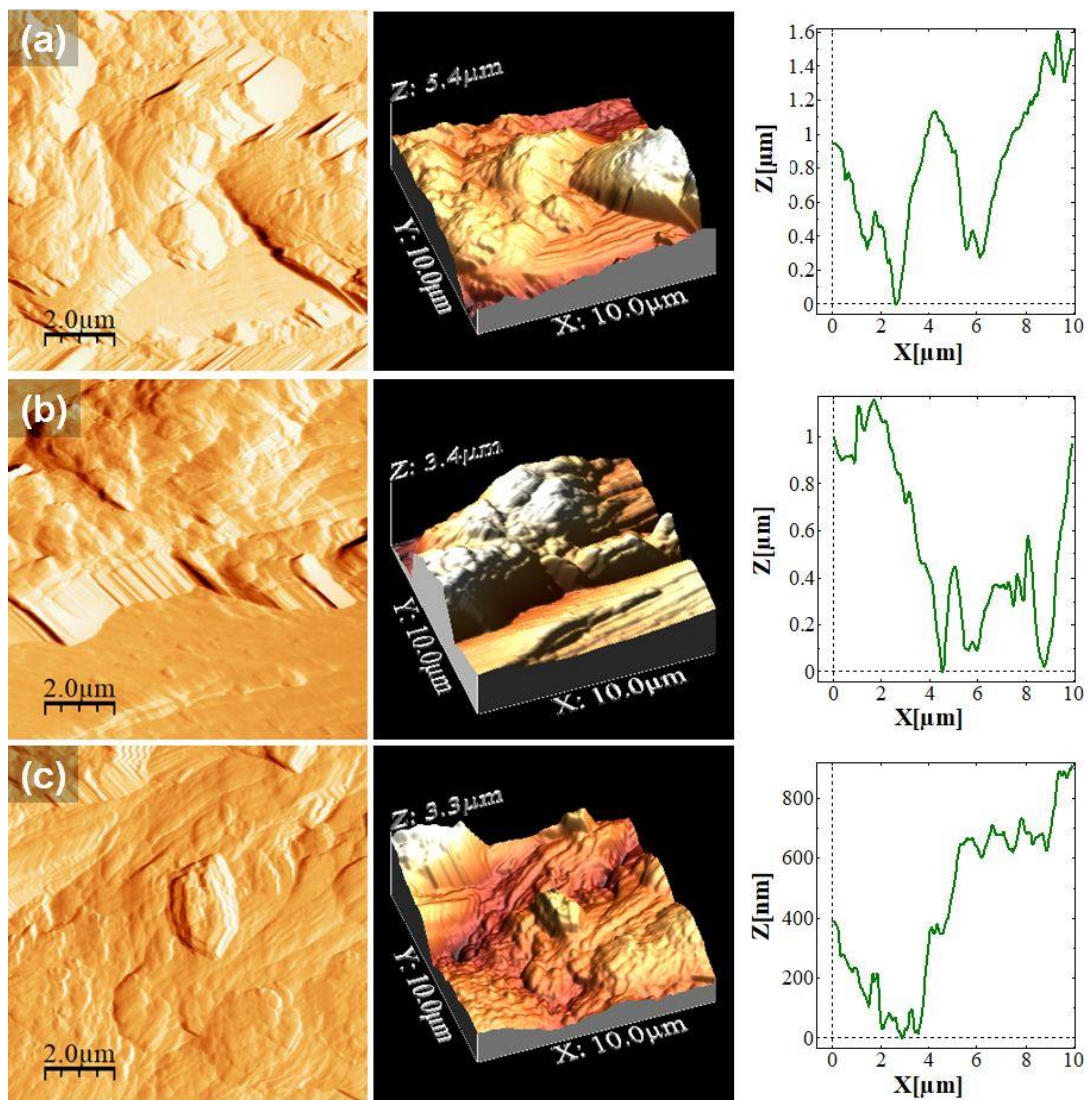


Figure 3. AFM topography images of Angelim Pedra cut in (a) Radial, (b) Tangential, and (c) Transverse directions. At right a line profile over these surfaces illustrates the height variation.

Figure 3 clearly shows that the values on the scale color are quite different among these samples, indicating the high roughness of the wood surface. Relative higher surface heights are observed in the R sample (Figure 3a) and this implies different roughness values as compared with Ta and Tr (Figure 3b and c). This standard image to assess wood or wood fiber was also used by Lahiji et al. (2010), whose appearance of the images presented is similar. They were developing the necessary protocols to use atomic force microscopy (AFM) technique to characterize cellulose nanocrystals mechanical properties and surface characteristics. Recently, some other study about the wood surface and natural fiber materials have been carried out to obtain localized surface energy information in submicron structures (Frybort, Obersiebnig, Müller, Gindl-Altmutter, & Konnerth, 2014; Jin & Kasal, 2016; Pietak, Korte, Tan, Downard, & Staiger, 2007; Raj, Balnois, Baley, & Grohens, 2009).

Roughness analysis

Figure 4 presents a graph of the roughness as a function of cut direction. It can be observed that both Rq and Ra have the same behavior. Rq varies from 42.35 ± 20.11 nm to 96.77 ± 27.97 nm and Ra varies from 33.61 ± 16.56 nm to 82.20 ± 23.96 nm per $10 \mu\text{m} \times 10 \mu\text{m}$ area.

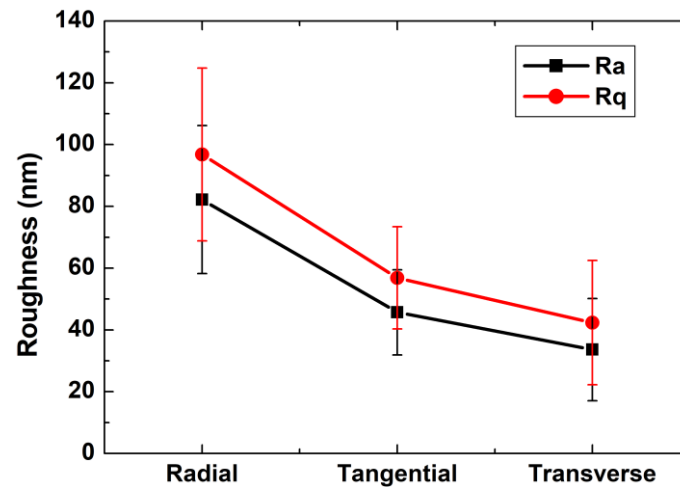


Figure 4. Graphic representation of Rq and Ra roughness as a function of R, Ta, and Tr.

Due to the irregularity of the processed wood surfaces, their cellular structure, and machining process, there are no standards for measuring wooden surfaces, which makes the application of standards unreliable (Funck, Forrer, Butler, Brunner, & Maristany, 1993; Krisch & Csiha, 1999). However, to determine the roughness of the wood surface, there are methodologies used in the industry which are based on visual and tactile senses and methods using surface measurement equipment (Fujiwara, Fujii, & Okumura, 2005).

On the other hand, in several publications measuring resolution and other important metrological data they are absent, what makes difficult to compare even the same type of processing. In general, profilometers (mechanical (probe) or light (laser) methods) are used to measure and calculate the roughness on areas around hundreds of square microns. As a consequence, it does not allow to distinguish places on the surface to create a pattern to perform measurements. Since sanding is an important process, it exposes specific characteristics of the interior of the wood that cannot be analyzed in detail by the equipment generally used. Nevertheless, the AFM can analyze reentrances resulting from cuts in the fibers and veins of wood on an atomic scale, generating images that allow comparisons to be made between different surface textures, and calculating roughness among other relevant surfaces such as skewness and kurtosis. That might be considered as a possible measurement standard as it evaluates specific regions that are restricted to other measurement techniques. A numerical evaluation of the surface quality implies the calculation of standard roughness parameters.

Conclusions

We have measured the roughness on wood surface with standard tips by AFM under specific environment conditions. It is shown that the surface roughness of wood varies according to the cut direction, in which the Radial has the highest values as compared with Tangential and Transverse. We also propose that the AFM technique could be used as a useful tool to measure and calculate roughness on specific surface regions, besides offering a submicrometrical image from wooden surfaces. The data set that can be provided by AFM can be of great use in species inspection of deforestation in the Amazon.

Acknowledgements

The authors thank CAPES (Coordination for the Improvement of Higher Education Personnel) for the financial support, as well as the use of the infrastructure of the Analytical Center of Universidade Federal do Amazonas (UFAM).

References

- Abouelatta, O. B., & Mádl, J. (2001). Surface roughness prediction based on cutting parameters and tool vibrations in turning operations. *Journal of Materials Processing Technology*, 118(1-3), 269–277. DOI: [https://doi.org/10.1016/S0924-0136\(01\)00959-1](https://doi.org/10.1016/S0924-0136(01)00959-1)
- Aguilera, A., & Muñoz, H. (2011). Rugosidad superficial y potencia de corte en el cepillado de *Acacia melanoxylon* y *sequoia sempervirens*. *Maderas Ciencia y Tecnología*, 13(1), 19–28. DOI: <https://doi.org/10.4067/S0718-221X2011000100002>
- Alday, E., Gómez, M., Ojeda, P., Caballero, M. L., & Moneo, I. (2005). IgE-mediated asthma associated with a unique allergen from Angelim pedra (*Hymenolobium petraeum*) wood. *The Journal of allergy and Clinical Immunology*, 115(3), 634–636. DOI: <https://doi.org/10.1016/j.jaci.2004.10.052>
- Botosso, P. C. (2009). *Identificação macroscópica de madeiras: guia prático e noções básicas para o seu reconhecimento*. Colombo, PR: Embrapa Florestas.
- Corrêa, M. P. (1984). *Dicionário das plantas úteis do Brasil e das exóticas cultivadas*. Rio de Janeiro, RJ: Instituto Brasileiro de Desenvolvimento Florestal.
- Csanády, E., Magoss, E., & Tolvaj, L. (2015). *Quality of Machined Wood Surfaces*. New York, NY: Springer International Publishing.
- Cybulska, J., Konstankiewicz, K., Zdunek, A., & Skrzypiec, K. (2010). Nanostructure of natural and model cell wall materials. *International Agrophysics*, 24(2), 107–114.
- Daniel, G. (2016). *Microscope techniques for understanding wood cell structure and biodegradation*. In Y. S. Kim, R. Funada & A. P. Singh (Eds.), *Secondary Xylem Biology: Origins, Functions, and Applications* (p. 309–343). Cambridge, MA: Academic Press.
- Ferreira, G. C., Gomes, J. I., & Hopkins, M. J. G. (2004). Estudo anatômico das espécies de *Leguminosae* comercializadas no estado do Pará como “angelim.” *Acta Amazonica*, 34(3), 387–398. DOI: <https://doi.org/10.1590/S0044-59672004000300005>
- Frybort, S., Obersriebnig, M., Müller, U., Gindl-Altmutter, W., & Konnerth, J. (2014). Variability in surface polarity of wood by means of AFM adhesion force mapping. *Colloids and Surfaces A Physicochemical and Engineering Aspects (Colloid Surface A)*, 457, 82–87. DOI: <https://doi.org/10.1016/j.colsurfa.2014.05.055>
- Fujiwara, Y., Fujii, Y., & Okumura, S. (2005). Relationship between roughness parameters based on material ratio curve and tactile roughness for sanded surfaces of two hardwoods. *Journal of Wood Science*, 51, 274–277. DOI: <https://doi.org/10.1007/s10086-004-0649-8>
- Funck, J. W., Forrer, J. B., Butler, D. A., Brunner, C. C., & Maristany, A. G. (1993). Measuring surface roughness on wood: a comparison of laser-scatter and stylus tracing approaches. In *Proceedings of the Volume 1821 – Applications in Optical science and Engineering*. In G. M. Brown, K. G. Harding & H. P. Stahl (Eds.), *Industrial Applications of Optical Inspection, Metrology, and Sensing* (p. 173–184).
- Gadelmawla, E. S., Koura, M. M., Maksoud, T. M. A., Elewa, I. M., & Soliman, H. H. (2002). Roughness parameters. *Journal of Materials Processing Technology*, 123(1), 133–145. DOI: [https://doi.org/10.1016/S0924-0136\(02\)00060-2](https://doi.org/10.1016/S0924-0136(02)00060-2)
- Ghisleni, R., Rzepiejewska-Malyska, K., Philippe, L., Schwaller, P., & Michler, J. (2009). In situ SEM indentation experiments: instruments, methodology, and applications. *Microscopy Research & Technique*, 72(3), 242–249. DOI: <https://doi.org/10.1002/jemt.20677>
- Gurau, L., Mansfield-Williams, H., & Irle, M. (2005). The influence of wood anatomy on evaluating the roughness of sanded solid wood. *Journal of the Institute of Wood Science*, 17(2), 65–74. DOI: <https://doi.org/10.1179/wsc.2005.17.2.65>
- Horcas, I., Fernández, R., Gómez-Rodríguez, J. M., Colchero, J., Gómez-Herrero, J. M., & Baro, A. M. (2013). WSXM : A software for scanning probe microscopy and a tool for nanotechnology. *Review of Scientific Instruments*, 78(1), 013705. DOI: <https://doi.org/10.1063/1.2432410>
- Jin, X., & Kasal, B. (2016). Adhesion force mapping on wood by atomic force microscopy: influence of surface roughness and tip geometry. *Royal Society Open Science*, 3(10), 160248. DOI: <https://doi.org/10.1098/rsos.160248>

- Kawasaki, M., Nobuchi, T., Nakafushi, Y., Nose, M., Shibata, M., Li, P., & Shiojiri, M. (2017). Structural observations and biomechanical measurements of clarinet reeds made from *Arundo donax*. *Microscopy Research & Technique*, 80(8), 959–968. DOI: <https://doi.org/10.1002/jemt.22889>
- Krisch, J., & Csiha, C. (1999). Analyzing wood surface roughness using an S3P perthometer and computer based data processing. In *Proceedings of the XIII Sesja Naukowa Badania Dla Meblarstwa Poland*, (p. 145-154).
- Lahiji, R. R., Xu, X., Reifenger, R., Raman, A., Rudie, A., and Moon, R. J. (2010). Atomic force microscopy characterization of cellulose nanocrystals. *Langmuir*, 26(6), 4480–4488. DOI <https://doi.org/10.1021/la903111j>.
- Lewis, G., Schrire, B., Mackinder, B., & Lock, M. (2005). *Legumes of the world*. London, UK: Royal Botanic Gardens Kew.
- Mainieri, C., & Primo, B. L. (1968). Madeiras denominadas “angelim”, estudo anatômico macro e microscópico. *Anuário Brasileiro de Economia Florestal*, 19, 39-87.
- Martins, V. A. (1988). *Secagem de madeira serrada*. Brasília, DF: IBDF.
- Melling, M., Karimian-Teherani, D., Mostler, S., Behnam, M., & Hochmeister, S. (2004). 3-D morphological characterization of the liver parenchyma by atomic force microscopy and by scanning electron microscopy. *Microscopy Research and Technique*, 64(1), 1–9. DOI: <https://doi.org/10.1002/jemt.20045>
- Moreschi, J.C. (2005). *Propriedades da madeira* (4a Ed.). Curitiba, PR: Ministério da Educação e do Desporto.
- Oliveira, L. Z. d., Cesarino, F., Pantoja, T. d. F., & Môro, F. V. (2010). Aspectos morfológicos de frutos, sementes, germinação e plântulas de *Hymenolobium petraeum*. *Ciência Rural*, 40(8), 1732–1740. DOI: <https://doi.org/10.1590/S0103-84782010000800010>
- Pietak, A., Korte, S., Tan, E., Downard, A., & Staiger, M. P. (2007). Atomic force microscopy characterization of the surface wettability of natural fibres. *Applied Surface Science*, 253(7), 3627–3635. DOI: <https://doi.org/10.1016/j.apsusc.2006.07.082>
- Raj, G., Balnois, E., Baley, C., & Grohens, Y. (2009). Adhesion force mapping of raw and treated flax fibres using AFM force-volume. *Journal of Scanning Probe Microscopy*, 4(2), 66–72. DOI: <https://doi.org/10.1166/jspm.2009.1010>
- Romagnolj, M., Sarlatto, M., Terranova, F., Bizzarri, E., & Cesetti, S. (2007). Wood identification in the Cappella Palatina ceiling (12th century) in Palermo (Sicily, Italy). *IAWA Journal*, 28(2), 109–124. DOI: <https://doi.org/10.1163/22941932-90001628>
- Thoma, H., Peri, L., & Lato, E. (2015). Evaluation of wood surface roughness depending on species characteristics. *Maderas Ciencia y Tecnología*, 17(2), 285–292. DOI: <https://doi.org/10.4067/S0718-221X2015005000027>
- Zhang, L., Chen, F., Yang, H., Ye, X., Sun, X., Liu, D., ... Deng, Y. (2012). Effect of temperature and cultivar on nanostructural changes of water-soluble pectin and chelate-soluble pectin in peaches. *Carbohydrate Polymers*, 87(1), 816–821. DOI: <https://doi.org/10.1016/j.carbpol.2011.08.074>